JOURNAL OF SPACECRAFT AND ROCKETS
Vol. 48, No. 2, March–April 2011

Electronic Energy Level Transition and Ionization Following the Quantum-Kinetic Chemistry Model

Derek S. Liechty*,†
NASA Langley Research Center, Hampton, Virgina 23681
and
Mark Lewis‡
University of Maryland, College Park, Maryland 20742

DOI: 10.2514/1.48826

A new method of treating electronic energy level transitions as well as linking ionization to electronic energy levels is proposed following the quantum-kinetic chemistry model of Bird. Although the use of electronic energy levels and ionization reactions in direct simulation Monte Carlo method are not new ideas, the current method of selecting what level to transition to, how to reproduce transition rates, and the linking of the electronic energy levels to ionization are, to the author's knowledge, novel concepts. The resulting equilibrium temperatures are shown to remain constant, and the electronic energy level distributions are shown to reproduce the Boltzmann distribution. The electronic energy level transition rates and ionization rates due to electron impacts are shown to reproduce theoretical and measured rates. The rates due to heavy particle impacts, while not as favorable as the electron impact rates, compare favorably to values from the literature. Thus, these new extensions to the quantum-kinetic chemistry model of Bird provide an accurate method for predicting electronic energy level transition and ionization rates in gases. Because these methods are not dependent upon any equilibrium rate equations or the macroscopic temperature of the gas, they are more appropriate for nonequilibrium flows.

Nomenclature

d	=	diameter of particle, m
$\mathrm{d}n$	=	number of transitions in sample
$\mathrm{d}t$	=	sample time, s
f	=	distribution function
g	=	energy level degeneracy
i, j, J	=	energy levels
k	=	Boltzmann's constant ($k = 1.3806503\mathrm{e}-23\ \mathrm{m^2\,kg\,s^{-2}\,K^{-1}}$)
k_f	=	forward reaction rate ($\mathrm{m^3/molecule/s}$)
l	=	orbital quantum number
L	=	total orbital angular momentum quantum number
m	=	mass, kg
N	=	number of molecules
n	=	number density ($1/\mathrm{m^3}$) and principal quantum number
P	=	probability
S	=	total spin quantum number
T	=	temperature, K
v_r	=	relative velocity in a collision, m/s
x	=	number of active electrons for an atomic level
Γ	=	gamma function
δ	=	Dirac delta
ε	=	energy, J
$\varepsilon_{\mathrm{tr}}$	=	translational energy ($\varepsilon_{\mathrm{tr}} = 0.5\ \mu v_r^2$)
Θ	=	characteristic temperature, K
μ	=	reduced mass in a collision ($\mu = m_1 m_2/(m_1 + m_2)$)
ω	=	exponent in variable hard sphere model

Subscripts

0, 1	=	ground and first electronic energy level
coll	=	collision value
diss	=	dissociation value
el	=	electronic energy component
heavy	=	heavy particle (atom/molecule)
i, j, J	=	energy levels
ion	=	ionization value
max	=	maximum value
pair	=	value obtained from both particles in collision
particle	=	value obtained from single particle in collision
ref	=	reference value
tr	=	translational energy component
vib	=	vibrational energy component

I. Introduction

AS WE consider missions, both manned and unmanned, where the (re)entry velocities result in shock-layer temperatures on the order of tens-of-thousands of degrees Kelvin, the importance of electronic energy levels and ionization reactions become more pronounced. Although the treatment of electronic energy levels and ionization reactions using the direct simulation Monte Carlo (DSMC) method is not a new development [1–3], most of these methods are based on measured, equilibrium rates, which are always questionable at high temperature, especially when applied to nonequilibrium problems. The primary reason for the inadequate state of chemical-reaction modeling is the difficulty in accurately measuring the internal energy state specific reaction rates to validate theoretical models in the temperature range of interest. Therefore, most reaction rates are based on low-temperature equilibrium measurements and are fit to the most reliable measured data sets. In some cases, the uncertainty associated with the spread of these measurements exceeds 1 order of magnitude [4].

To model internal energy exchange phenomenon and chemical reactions using the DSMC method, complete tabulations of the cross sections as functions of the impact parameters and energy states of

Presented as Paper 2010-449 at the 48th AIAA Aerospace Sciences Meeting Including The New Horizons Forum And Aerospace Exposition, Orlando, FL, 4–7 January 2010; received 6 January 2010; revision received 22 October 2010; accepted for publication 5 December 2010.

*Aerospace Engineer, Aerothermodynamics Branch, MS 408A. Member AIAA.
†Graduate Student, University of Maryland, Aerospace Engineering.
‡Professor, Aerospace Engineering, Room 3179 Martin Hall. Fellow AIAA, President-Elect AIAA.

the molecules are ideally needed. Such information could come from quantum-mechanical calculations, supported by experiment. However, very little such information is available and that limited information applies to only a small number of reactions. In the absence of such detailed data, DSMC simulations resort to phenomenological models that capture the most essential features of the microscopic mechanisms while maintaining the computational efficiency of DSMC. The algorithms outlined herein are of this class of model and are also bound to any physical limitations that come under any assumptions made in the standard DSMC algorithms.

Recently, an approach for determining chemical-reaction rates from microscopic molecular data, referred to as the quantum-kinetic chemistry model (QK), has been developed [5,6] that does not use any macroscopic rate information. It is the purpose of this paper to introduce a new method of treating electronic energy level transitions following the QK methodologies. One distinct feature of the QK is the direct linking of the vibrational energy level of a molecule to the dissociation of that molecule. This idea is extended in this paper to the direct linking of the electronic energy level of an atom/molecule to ionization. These methodologies, since they do not rely on any equilibrium-based or macroscopic data, are more appropriate for the rarefied, nonequilibrium flows of interest in atmospheric (re)entry.

II. Detailed Electronic Energy Level Model for DSMC

To implement a model for the distribution of electronic energy in the DSMC technique, there are three procedures that must be defined. First, when a particle is first introduced into a simulation, it is necessary to obtain a new electronic energy from a given distribution through statistical sampling. This is also required when a particle changes its electronic energy after a collision with a surface. Under equilibrium conditions, the distribution has the well known Boltzmann form. Second, it is necessary to statistically sample a new electronic energy following a collision which involves electronic energy transfer. Finally, a method to reproduce the electronic energy transition rate must be defined. In the following subsections, each of these tasks are considered.

A. Equilibrium Sampling

Each electronic energy level j has a distinct energy ε_j and degeneracy g_j. The Boltzmann distribution for the electronic energy levels at a given temperature T gives the following result for the fraction of particles in level j:

$$f_{\mathrm{el}}(j) = \frac{N_j}{N} = \frac{g_j \exp(-\varepsilon_j/kT)}{\sum_{i=0}^{i_{\max}} g_i \exp(-\varepsilon_i/kT)} \tag{1}$$

This distribution is used when creating a new particle in the DSMC simulation at a boundary specified at the temperature T. However, it is not possible to sample an electronic energy level j directly from the distribution. Therefore, an acceptance-rejection procedure is used. This is performed by selecting values for j from the following distribution:

$$f'_{\mathrm{el}}(j) = \frac{g_j \exp(-\varepsilon_j/kT)}{g_J \exp(-\varepsilon_J/kT)} \tag{2}$$

where J is the value of j for which Eq. (1) is a maximum. Unfortunately, since the degeneracy of each level is a variable specific to each species, there is no way to know a priori what level is going to give the maximum, so the maximum level must be searched for at each implementation or saved for a constant boundary temperature. The sampling of a new electronic energy level then proceeds as follows:

1) Select at random an electronic energy level evenly distributed between 0 and $J_{\max}$, where $J_{\max}$ is the maximum possible energy level. A random number, RAND_1, evenly distributed between 0 and 1 is needed such that:

$$j = \mathrm{int}[(1 + J_{\max}) * \mathrm{RAND}_1] \tag{3}$$

2) Determine the value J for which Eq. (1) is a maximum;

3) Accept the value of j if $f'_{\mathrm{el}}(j) > \mathrm{RAND}_2$;

4) If the value of j is not accepted, then return to step 1.

B. Postcollision Sampling

A phenomenological approach is usually adopted in the DSMC method when a collision occurs that involves energy transfer. The Borgnakke–Larsen method [7] samples a postcollision state from a combined distribution of the translational and electronic collision energies of the colliding particles. Based on the approach of Bergemann and Boyd [8] and Boyd [9], the Dirac delta is used to write the distribution of energies in Eq. (1) in the following continuous form:

$$f_{\mathrm{el}}(\varepsilon_{\mathrm{el}}, j) = \frac{g_j \exp(-\varepsilon_j/kT)}{\sum_{i=0}^{i_{\max}} g_i \exp(-\varepsilon_i/kT)} \delta(\varepsilon_{\mathrm{el}}/kT - \varepsilon^j_{\mathrm{el}}/kT) \tag{4}$$

Consideration must now be given to the distribution of translational energy of the colliding particles. This distribution is naturally affected by the intermolecular model used since this determines the collision probability. For the present study, the variable hard sphere (VHS) collision model of Bird [10] is used. However, it is a simple matter to develop the formulation for an alternative collision model such as the variable soft sphere of Koura and Matsumoto [11]. For the VHS model, the distribution of the translational collision energies is:

$$f_{\mathrm{tr}}(\varepsilon_{\mathrm{tr}}) = \frac{1}{\Gamma(5/2 - \omega)} (\varepsilon_{\mathrm{tr}}/kT)^{3/2-\omega} \exp(-\varepsilon_{\mathrm{tr}}/kT) \tag{5}$$

Using Eqs. (4) and (5), the combined distribution for sampling a postcollision electronic energy level j' from the total collision energy $\varepsilon_{\mathrm{coll}} = \varepsilon_{\mathrm{tr}} + \varepsilon_{\mathrm{el}} = \varepsilon'_{\mathrm{tr}} + \varepsilon'_{\mathrm{el}}$ is:

$$f(j'; \varepsilon_{\mathrm{coll}}) = \frac{1}{\Gamma(5/2 - \omega)} \frac{g_j}{\sum_{i=0}^{i_{\max}} g_i \exp(-\varepsilon_i/kT)} \times [(\varepsilon_{\mathrm{coll}} - \varepsilon'_{\mathrm{el}})/kT]^{3/2-\omega} \exp(-\varepsilon_{\mathrm{coll}}/kT) \tag{6}$$

In applying the general Borgnakke–Larsen scheme, it is assumed that local thermodynamic equilibrium prevails. Therefore, the temperature T in Eq. (6) is constant. Also, the total collision energy is constant, so it is only necessary to perform sampling of the postcollision state from the following distribution form:

$$g(j'; \varepsilon_{\mathrm{coll}}) \propto g_{j'} (\varepsilon_{\mathrm{coll}} - \varepsilon^{j'}_{\mathrm{el}})^{3/2-\omega} \tag{7}$$

Again, an acceptance-rejection procedure is used. The normalized distribution that is required is obtained by finding the value of j' for which Eq. (7) is maximum, J', which is different for each value of $\varepsilon_{\mathrm{coll}}$. Therefore, the following distribution is obtained:

$$g'(j'; \varepsilon_{\mathrm{coll}}) = \frac{g_{j'} (\varepsilon_{\mathrm{coll}} - \varepsilon^{j'}_{\mathrm{el}})^{3/2-\omega}}{g_{J'} (\varepsilon_{\mathrm{coll}} - \varepsilon^{J'}_{\mathrm{el}})^{3/2-\omega}} \tag{8}$$

In the DSMC code, these procedures are implemented in the following way:

1) Given a pair of particles with total collision energy $\varepsilon_{\mathrm{coll}}$ which undergoes electronic energy exchange, determine J'.

2) Determine the maximum allowable electronic energy level obtainable from $\varepsilon_{\mathrm{coll}}$, J''.

3) Take J^* to be the smaller of J' and J''.

4) As described in the previous section on equilibrium sampling, perform an acceptance-rejection procedure to sample j' from:

$$g'(j'; \varepsilon_{\mathrm{coll}}) = \frac{g_{j'} (\varepsilon_{\mathrm{coll}} - \varepsilon^{j'}_{\mathrm{el}})^{3/2-\omega}}{g_{J^*} (\varepsilon_{\mathrm{coll}} - \varepsilon^{J^*}_{\mathrm{el}})^{3/2-\omega}} \tag{9}$$

C. Electronic Energy Level Transitions

A transition from electronic energy level i to level j for atomic nitrogen, N, can be written in the form of a chemical reaction as:

$$N^i + M \rightarrow N^j + M \tag{10}$$

Following the QK, the simplest model is to assume that the transition occurs if the electronic energy level of N after a trial Borgnakke–Larsen redistribution of the collision energy is $j^* = j$. Since we are treating the transition as a chemical reaction, there are $J_{\max}$ transitions to consider where $J_{\max}$ is the maximum energy level energetically possible. There is a possibility that there will be multiple transitions where $j^* = j$, each of which, according to the QK, are equally probable. In the DSMC code, the decision to transition from level i to j is implemented in the following way:

1) Check each transition i to j from $j = 0$ to $J_{\max}$, performing a trial Borgnakke–Larsen redistribution for each, keeping a list of the possible reactions ($j^* = j$).

2) If there are any possible transitions from step 1, choose a random transition from the list and perform the transition.

III. Linking Ionization to Electronic Energy Levels in DSMC

Bird [5] proposed a set of molecular-level chemistry models based solely on fundamental properties of the two colliding molecules: their total collision energy, quantized vibrational energy levels, and molecular dissociation energies. These models link chemical-reaction cross sections to the energy exchange process and the probability of transition between vibrational energy states. The Borgnakke–Larsen procedures and the principle of microscopic reversibility are then used to derive simple models for recombination reactions and for the reverse (exothermic) reactions. These models do not require any macroscopic data, and they function by seeking to balance the fluxes into and out of each state, thus satisfying microscopic reversibility.

In this section, these ideas are extended to include the quantized electronic energy levels and molecular/atomic ionization energies. For dissociation to occur for an ionization reaction written as $A + M \rightarrow A^+ + M$, if the collision energy:

$$\varepsilon_{\text{coll}} = \varepsilon_{\text{tr,pair}} + \varepsilon_{\text{vib,particle}} \tag{11}$$

exceeds the dissociation energy, the molecule in question dissociates. If this is extended to electronic energy levels and ionization, if the collision energy now defined as:

$$\varepsilon_{\text{coll}} = \varepsilon_{\text{tr,pair}} + \varepsilon_{\text{el,particle}} \tag{12}$$

exceeds the ionization energy, the particle in question loses an electron, becoming an ion.

IV. Results

In this section, the new electronic energy exchange, electronic energy level transition, and ionization reaction models are applied in a two-dimensional DSMC code where the results are accumulated over all cells to approximate a zero-dimensional simulation. The test gas is composed of molecular and atomic nitrogen, N_2 and N, and electrons, e, where the relevant simulation parameters are listed in Table 1. A list of electronic energy levels for N_2 and N are presented in Tables A1 and A2 in the Appendix, respectively. The simulations were run at varying temperatures between 10,000 and 60,000 K at a number density of $1e23/\text{m}^3$ in an adiabatic box 0.002 m on a side with 300,000 molecules. The initial molecular electronic energy levels were initialized by sampling as described above using the values listed in the Appendix. During the simulations, relaxation of the internal energy modes of the particles was allowed to proceed as usual, but when a reaction was determined to take place, the number of reactions was advanced by one but the simulators were left unchanged, so no energy was added to or taken away from the flow. In the figures included in this section, the solid lines are values from quoted rates from the literature, and the symbols are the values that were sampled from DSMC.

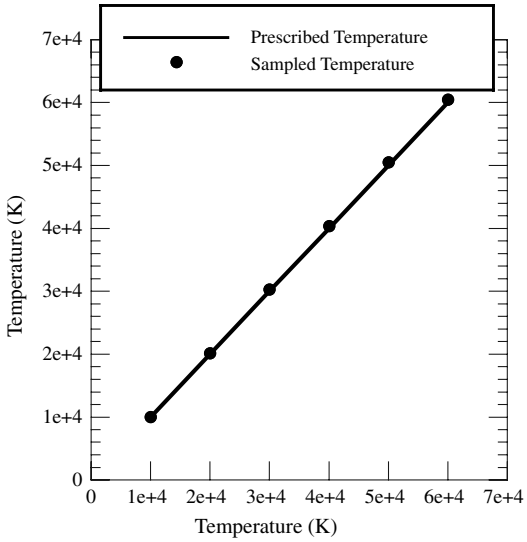

Fig. 1 Sampled translational temperature over a range of input equilibrium temperatures.

In order for these procedures to be acceptable, they need to reproduce equilibrium conditions after the simulation has been allowed to run for a sufficient amount of time to ensure that detailed balance has been enforced. The first requirement is for the procedures to remain at the input equilibrium temperature. The input equilibrium temperature is compared with the sampled translational temperature in Fig. 1 and can be seen to remain constant. The resultant population distribution over the first 20 energy levels for a range of temperatures is compared with the Bolzmann distribution in Fig. 2. Again, the simulation represents the equilibrium state very well.

Sampled transition rates will now be compared with those found in literature. We must first define how to measure the sampled transition rates in DSMC. The transition rate for the reaction shown in Eq. (10) is calculated as:

$$k_f = \frac{\frac{\mathrm{d}n_{N^i}}{\mathrm{d}t}}{n_{N^i} n_N} \tag{13}$$

where the numerator is the change in the number density of level i due to the reaction in the sampled time.

Electron Impact Rates: We will begin by examining electronic energy level transitions caused by electron impacts. Sampled transition rates are compared with those by Chernyi and Losev [12] in Fig. 3 for molecular nitrogen. The sampled rates very nearly match the values quoted in the literature. Sampled electron impact electronic energy level transition rates for atomic nitrogen are compared in Fig. 4 with values from Frost et al. [13] with similar results.

Table 1 Gas properties

Test gas	d_{ref}, m	m (kg)	T_{ref}, K	ω	Θ_{vib}, K	Z_{ref}	Θ_{diss}, K	ε_{ion}, J
N_2	3.580E − 10	4.650E − 26	1000	0.68	3371.0	52500	113500	2.496192E − 18
N	3.110E − 10	2.325E − 26	1000	0.65	-	-	-	2.327964E − 18
e	5.640E − 15	9.109E − 31	1000	0.60	-	-	-	-

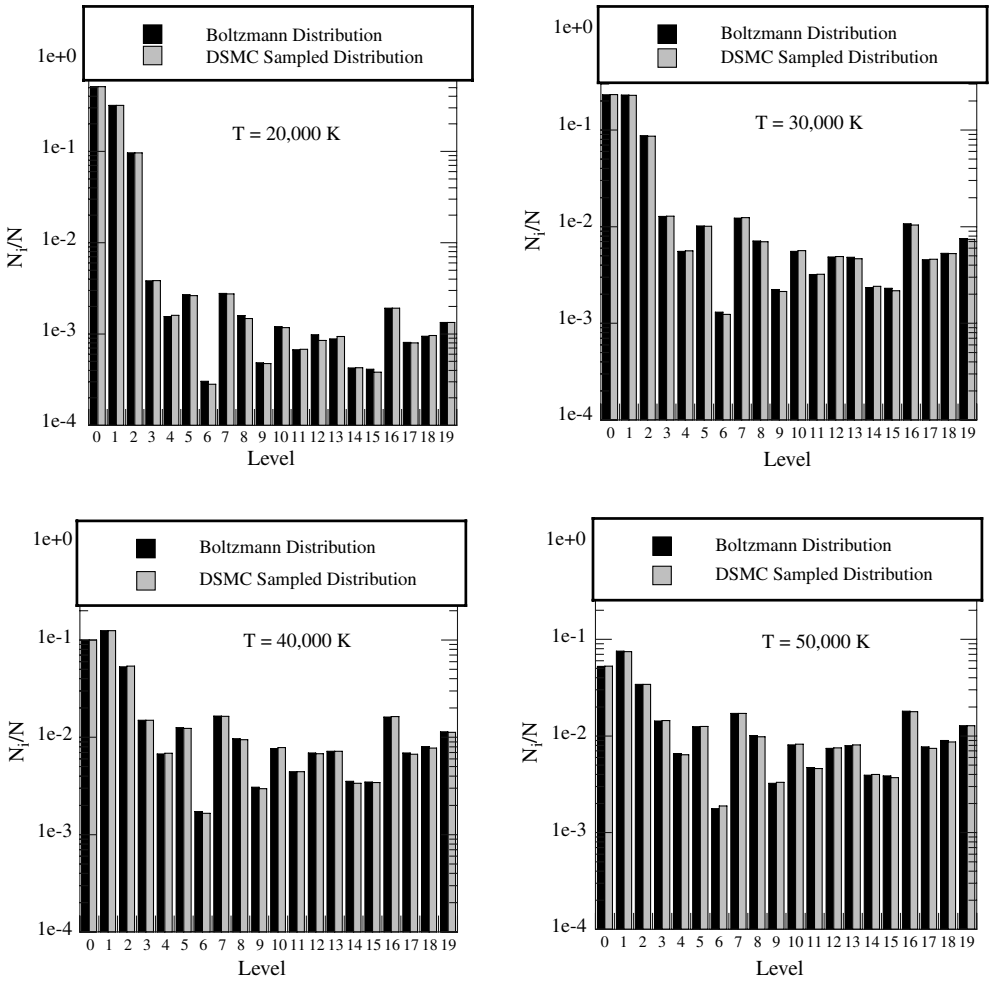

Fig. 2 Sampled electronic energy level distributions for the first 20 levels of atomic Nitrogen over a range of equilibrium temperatures.

Next, electron impact ionization rates will be compared for both atomic and molecular nitrogen. Figure 5 presents a comparison between the sampled rates and those from Losev et al. [14] for molecular nitrogen while Fig. 6 compares the rates between DSMC and a variety of sources [4,14–19] for electron impact ionization rates for atomic nitrogen. As with the electronic energy level transition rates for electron impact, the ionization rates compare well with literature.

Heavy Particle Impact Rates: Using the current model for electronic energy level transitions and ionization, the comparison between rates measured using DSMC and those from the literature for heavy particle impacts are not as similar as those for electron impacts. Sampled heavy particle impact endothermic electronic energy level transition rates for molecular nitrogen are compared with those of Park [20] in Fig. 7. The measured trends match those from the literature for individual level transitions, but the magnitudes are different, especially for the level 0 to 1 transition for a $N_2 + N_2$ collision. The other transition rates are approximately within an order of magnitude of the quoted rates, but the comparison is not as good as

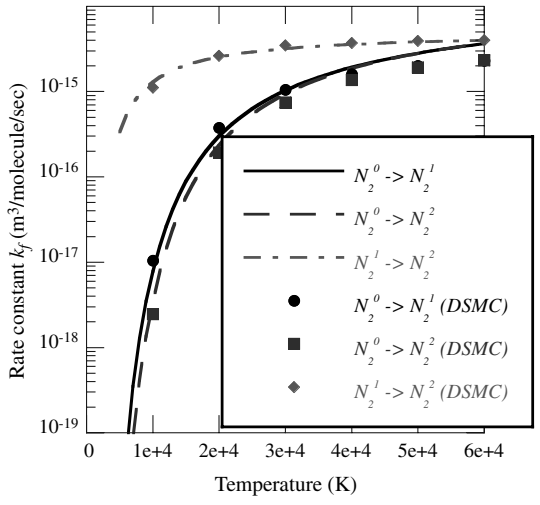

Fig. 3 Electron impact electronic energy transition rates for N_2.

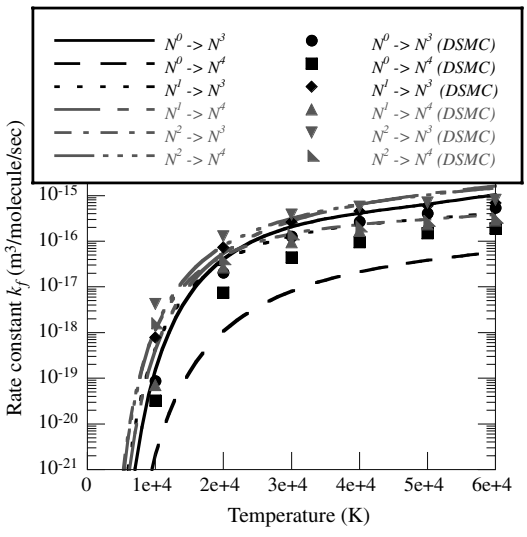

Fig. 4 Electron impact electronic energy transition rates for N.

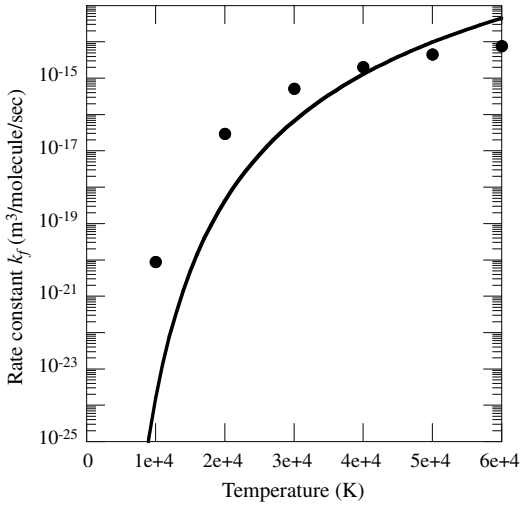

Fig. 5 Electron impact ionization rates for N_2.

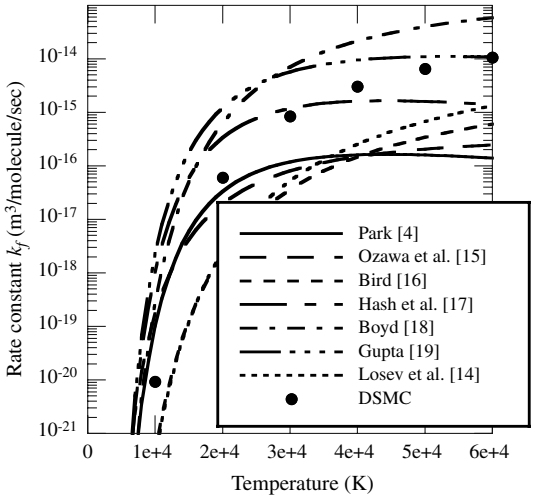

Fig. 6 Electron impact ionization rates for N.

the electron impact transition rates. Sampled heavy particle impact exothermic electronic energy level transition rates for N_2 are compared with those of Guerra and Loureiro [21] in Fig. 8. The quenching transitions are much closer to the measured rates as compared with the excitation transitions. This is most likely due to the fact that it is the quenching rates that are measured in the laboratory. The excitation rates are then calculated assuming equilibrium. It is possible that the transitions in the laboratory are not at equilibrium, therefore some of the rates are farther off than others.

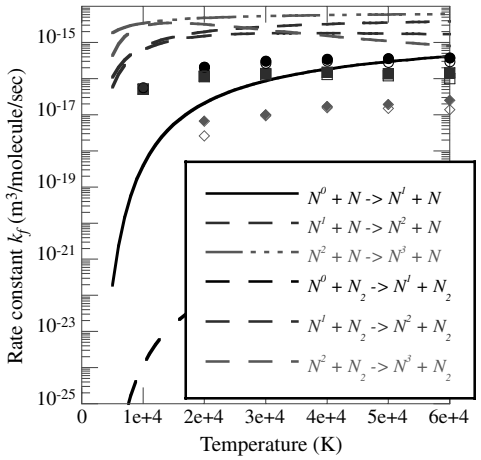

Fig. 7 Heavy particle impact electronic energy level endothermic transition rates for N_2.

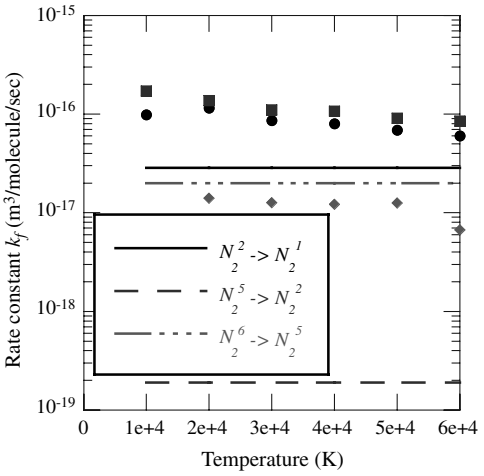

Fig. 8 Heavy particle impact electronic energy level exothermic transition rates for N_2.

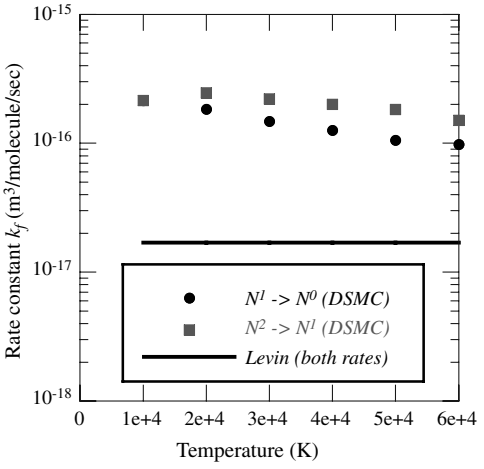

Fig. 9 Heavy particle impact electronic energy level exothermic transition rates for N.

When examining atomic nitrogen heavy particle impact electronic energy level transition rates, only quenching transition rates were found for comparison to the sampled rates. The sampled rates are compared with values quoted by Levin [22] in Fig. 9. Once again the quenching rates for electronic energy transitions compare reasonably well. Heavy particle impact ionization rates are not prevalent in the literature, so are not included in this analysis.

V. Conclusions

Kinetic theory-based chemical-reaction models recently proposed for the DSMC method have been extended to include electronic energy level transitions as well as ionization. This new set of models do not use measured macroscopic reaction/transition rates to calibrate adjustable parameters. Instead, they make use of the principles of microscopic reversibility and molecular-level energy exchange to predict the probability that a chemical reaction or energy level transition occurs during a collision between two particles.

Procedures have been defined that are required to implement the current model for the distribution of electronic energy in the DSMC technique. These include defining methods to sample from an equilibrium (Boltzmann) distribution, to sample postcollision states from a combined distribution of the translational and electronic

collision energies of the colliding particles, and to determine when a particle should transition electronic energy levels. The first two methods are straight forward and can be derived following methods for other energy modes. The latter method is a novel implementation of the new chemical-reaction models. These three methods have been shown to maintain equilibrium temperatures and reproduce the Boltzmann distribution of electronic energy levels after sufficient simulation time. Sampled electronic energy transition rates have been shown to compare well to values from literature for electron impact transitions and reasonably well for heavy particle impact transitions.

The new chemical-reaction models have also been extended to include ionization reactions. Following the new dissociation model, where a molecule dissociates if the available collision energy exceeds the dissociation energy, a particle will lose an electron if the available collision energy exceeds the ionization energy. The sampled ionization rates have been shown to agree well with values from literature for electron impact reactions. However, heavy particle ionization data are scarce in literature and have been excluded from the current study.

These new methodologies are a first step toward the realistic simulation of rarefied, hyper-velocity atmospheric (re)entry where nonequilibrium effects become important and equilibrium-based rate equations become questionable at best. The next logical step now that the electronic energy level transition rates can be accurately simulated is to include radiation, either directly (coupled) or indirectly (pass to a nonequilibrium radiation solver), as part of the DSMC solution. For the ionization reactions, some methodology must be implemented to accurately simulate the motion of the resultant plasma. These next steps are important and the method of their application must be carefully weighed such that the salient physics are captured.

Appendix

Table A1 Listing of electronic energy level information of molecular nitrogen

Level j	$\varepsilon_{\mathrm{el},j}$, J	g_j
0	0.00000	1
1	9.9726950E − 19	3
2	1.1843030E − 18	6
3	1.1880540E − 18	6
4	1.3164670E − 18	3
5	1.3538160E − 18	1
6	1.3762700E − 18	2
7	1.4482750E − 18	2
8	1.5414820E − 18	5
9	1.6924570E − 18	1
10	1.7242390E − 18	6
11	1.7706570E − 18	6
12	1.8473930E − 18	10
13	1.9388470E − 18	6
14	2.0778240E − 18	6

Table A2 Listing of electronic energy level information of atomic nitrogen

Level j	$\varepsilon_{\mathrm{el},j}$, J	g_j	n_j	l_j	x_j	S_j	L_j	Configuration	Term
0	0.00000	4	2	1	3	3/2	0	$2s^2 2p^3$	^{4}S°
1	3.8195294E − 19	10	2	1	3	1/2	2	$2s^2 2p^3$	^{2}D°
2	5.7287486E − 19	6	2	1	3	1/2	1	$2s^2 2p^3$	^{2}P°
3	1.6554172E − 18	12	3	0	1	3/2	1	$2s^2 2p^2(^3\mathrm{P})3s$	^{4}P
4	1.7121737E − 18	6	3	0	1	1/2	1	$2s^2 2p^2(^3\mathrm{P})3s$	^{2}P
5	1.7507040E − 18	12	2	1	4	3/2	1	$2s 2p^4$	^{4}P
6	1.8589476E − 18	2	3	1	1	1/2	0	$2s^2 2p^2(^3\mathrm{P})3p$	^{2}S°
7	1.8839019E − 18	20	3	1	1	3/2	2	$2s^2 2p^2(^3\mathrm{P})3p$	^{4}D°
8	1.8972523E − 18	12	3	1	1	3/2	1	$2s^2 2p^2(^3\mathrm{P})3p$	^{4}P°
9	1.9219038E − 18	4	3	1	1	3/2	0	$2s^2 2p^2(^3\mathrm{P})3p$	^{4}S°
10	1.9235458E − 18	10	3	1	1	1/2	2	$2s^2 2p^2(^3\mathrm{P})3p$	^{2}D°
11	1.9426247E − 18	6	3	1	1	1/2	1	$2s^2 2p^2(^3\mathrm{P})3p$	^{2}P°
12	1.9797645E − 18	10	3	0	1	1/2	2	$2s^2 2p^2(^1\mathrm{D})3s$	^{2}D
13	2.0598225E − 18	12	4	0	1	3/2	1	$2s^2 2p^2(^3\mathrm{P})4s$	^{4}P
14	2.0697973E − 18	6	4	0	1	1/2	1	$2s^2 2p^2(^3\mathrm{P})4s$	^{2}P
15	2.0783847E − 18	6	3	2	1	1/2	1	$2s^2 2p^2(^3\mathrm{P})3d$	^{2}P
16	2.0801974E − 18	28	3	2	1	3/2	3	$2s^2 2p^2(^3\mathrm{P})3d$	^{4}F
17	2.0827249E − 18	12	3	2	1	3/2	1	$2s^2 2p^2(^3\mathrm{P})3d$	^{4}P
18	2.0828065E − 18	14	3	2	1	1/2	3	$2s^2 2p^2(^3\mathrm{P})3d$	^{2}F
19	2.0859128E − 18	20	3	2	1	3/2	2	$2s^2 2p^2(^3\mathrm{P})3d$	^{4}D
20	2.0884332E − 18	10	3	2	1	1/2	2	$2s^2 2p^2(^3\mathrm{P})3d$	^{2}D
21	2.1151235E − 18	2	4	1	1	1/2	0	$2s^2 2p^2(^3\mathrm{P})4p$	^{2}S°
22	2.1219883E − 18	20	4	1	1	3/2	2	$2s^2 2p^2(^3\mathrm{P})4p$	^{4}D°
23	2.1257740E − 18	12	4	1	1	3/2	1	$2s^2 2p^2(^3\mathrm{P})4p$	^{4}P°
24	2.1299658E − 18	10	4	1	1	1/2	2	$2s^2 2p^2(^3\mathrm{P})4p$	^{2}D°
25	2.1343488E − 18	4	4	1	1	3/2	0	$2s^2 2p^2(^3\mathrm{P})4p$	^{4}S°
26	2.1377136E − 18	6	4	1	1	1/2	1	$2s^2 2p^2(^3\mathrm{P})4p$	^{2}P°
27	2.1827900E − 18	12	5	0	1	3/2	1	$2s^2 2p^2(^3\mathrm{P})5s$	^{4}P
28	2.1867017E − 18	6	5	0	1	1/2	1	$2s^2 2p^2(^3\mathrm{P})5s$	^{2}P
29	2.1896284E − 18	6	4	2	1	1/2	1	$2s^2 2p^2(^3\mathrm{P})4d$	^{2}P
30	2.1901014E − 18	28	4	2	1	3/2	3	$2s^2 2p^2(^3\mathrm{P})4d$	^{4}F
31	2.1916419E − 18	12	4	2	1	3/2	1	$2s^2 2p^2(^3\mathrm{P})4d$	^{4}P
32	2.1916419E − 18	14	4	2	1	1/2	3	$2s^2 2p^2(^3\mathrm{P})4d$	^{2}F
33	2.1920256E − 18	14	4	4	1	1/2	3	$2s^2 2p^2(^3\mathrm{P})4f\mathrm{D}$	$^2[3]^0$
34	2.1927445E − 18	14	4	4	1	1/2	3	$2s^2 2p^2(^3\mathrm{P})4f\mathrm{G}$	$^2[3]^0$
35	2.1930233E − 18	20	4	2	1	3/2	2	$2s^2 2p^2(^3\mathrm{P})4d$	^{4}D
36	2.1930782E − 18	18	4	4	1	1/2	4	$2s^2 2p^2(^3\mathrm{P})4f\mathrm{G}$	$^2[4]^0$
37	2.1931259E − 18	10	4	4	1	1/2	2	$2s^2 2p^2(^3\mathrm{P})4f\mathrm{D}$	$^2[2]^0$
38	2.1942236E − 18	6	4	4	1	1/2	1	$2s^2 2p^2(^3\mathrm{P})4f\mathrm{D}$	$^2[1]^0$

(continued)

Table A2 Listing of electronic energy level information of atomic nitrogen (Continued)

Level j	$\varepsilon_{\mathrm{el},j}$, J	g_j	n_j	l_j	x_j	S_j	L_j	Configuration	Term
39	2.1942468E − 18	10	4	2	1	1/2	2	$2s^2 2p^2(^3\mathrm{P})4d$	^{2}D
40	2.1944891E − 18	22	4	4	1	1/2	5	$2s^2 2p^2(^3\mathrm{P})4f$G	$^2[5]^0$
41	2.1947443E − 18	10	4	4	1	1/2	2	$2s^2 2p^2(^3\mathrm{P})4f$F	$^2[2]^0$
42	2.1949910E − 18	14	4	4	1	1/2	3	$2s^2 2p^2(^3\mathrm{P})4f$F	$^2[3]^0$
43	2.1950570E − 18	18	4	4	1	1/2	4	$2s^2 2p^2(^3\mathrm{P})4f$F	$^2[4]^0$
44	2.1957241E − 18	10	3	1	1	1/2	2	$2s^2 2p^2(^1\mathrm{D})3p$	^{2}D°
45	2.1992586E − 18	14	3	1	1	1/2	3	$2s^2 2p^2(^1\mathrm{D})3p$	^{2}F°
46	2.2061644E − 18	2	5	1	1	1/2	0	$2s^2 2p^2(^3\mathrm{P})5p$	^{2}S°
47	2.2090956E − 18	6	5	1	1	1/2	1	$2s^2 2p^2(^3\mathrm{P})5p$	^{2}P°
48	2.2091778E − 18	20	5	1	1	3/2	2	$2s^2 2p^2(^3\mathrm{P})5p$	^{4}D°
49	2.2092125E − 18	12	5	1	1	3/2	1	$2s^2 2p^2(^3\mathrm{P})5p$	^{4}P°
50	2.2149140E − 18	4	5	1	1	3/2	0	$2s^2 2p^2(^3\mathrm{P})5p$	^{4}S°
51	2.2225265E − 18	10	5	1	1	1/2	2	$2s^2 2p^2(^3\mathrm{P})5p$	^{2}D°
52	2.2310009E − 18	6	3	1	1	1/2	1	$2s^2 2p^2(^1\mathrm{D})3p$	^{2}P°
53	2.2374954E − 18	12	6	0	1	3/2	1	$2s^2 2p^2(^3\mathrm{P})6s$	^{4}P
54	2.2391604E − 18	6	6	0	1	1/2	1	$2s^2 2p^2(^3\mathrm{P})6s$	^{2}P
55	2.2407743E − 18	6	5	2	1	1/2	1	$2s^2 2p^2(^3\mathrm{P})5d$	^{2}P
56	2.2408504E − 18	28	5	2	1	3/2	3	$2s^2 2p^2(^3\mathrm{P})5d$	^{4}F
57	2.2412458E − 18	14	5	3	1	1/2	3	$2s^2 2p^2(^3\mathrm{P}_0)5f$	$^2[3]^0$
58	2.2414379E − 18	12	5	2	1	3/2	1	$2s^2 2p^2(^3\mathrm{P})5d$	^{4}P
59	2.2418528E − 18	14	5	2	1	1/2	3	$2s^2 2p^2(^3\mathrm{P})5d$	^{2}F
60	2.2420758E − 18	14	5	3	1	1/2	3	$2s^2 2p^2(^3\mathrm{P}_1)5f$	$^2[3]^0$
61	2.2422583E − 18	18	5	3	1	1/2	4	$2s^2 2p^2(^3\mathrm{P}_1)5f$	$^2[4]^0$
62	2.2423070E − 18	10	5	3	1	1/2	2	$2s^2 2p^2(^3\mathrm{P}_1)5f$	$^2[2]^0$
63	2.2428934E − 18	20	5	2	1	3/2	2	$2s^2 2p^2(^3\mathrm{P})5d$	^{4}D
64	2.2434580E − 18	10	5	2	1	1/2	2	$2s^2 2p^2(^3\mathrm{P})5d$	^{2}D
65	2.2436230E − 18	6	5	3	1	1/2	1	$2s^2 2p^2(^3\mathrm{P}_2)5f$	$^2[1]^0$
66	2.2437593E − 18	22	5	3	1	1/2	4.5	$2s^2 2p^2(^3\mathrm{P}_2)5f$	$^2[9/2]^0$
67	2.2438446E − 18	10	5	3	1	1/2	2	$2s^2 2p^2(^3\mathrm{P}_2)5f$	$^2[2]^0$
68	2.2439954E − 18	14	5	3	1	1/2	3	$2s^2 2p^2(^3\mathrm{P}_2)5f$	$^2[3]^0$
69	2.2440307E − 18	18	5	3	1	1/2	4	$2s^2 2p^2(^3\mathrm{P}_2)5f$	$^2[4]^0$
70	2.2515070E − 18	14	6	1	1	3/2	2	$2s^2 2p^2(^3\mathrm{P})6p$	^{4}D°
71	2.2522583E − 18	10	6	1	1	3/2	1	$2s^2 2p^2(^3\mathrm{P})6p$	^{4}P°
72	2.2665626E − 18	12	7	0	1	3/2	1	$2s^2 2p^2(^3\mathrm{P})7s$	^{4}P
73	2.2679643E − 18	14	6	3	1	1/2	3	$2s^2 2p^2(^3\mathrm{P}_0)6f$	$^2[3]^0$
74	2.2680191E − 18	6	6	2	1	1/2	1	$2s^2 2p^2(^3\mathrm{P})6d$	^{2}P
75	2.2680197E − 18	6	7	0	1	1/2	1	$2s^2 2p^2(^3\mathrm{P})7s$	^{2}P
76	2.2682030E − 18	28	6	2	1	3/2	3	$2s^2 2p^2(^3\mathrm{P})6d$	^{4}F
77	2.2686007E − 18	12	6	2	1	3/2	1	$2s^2 2p^2(^3\mathrm{P})6d$	^{4}P
78	2.2688525E − 18	14	6	3	1	1/2	3	$2s^2 2p^2(^3\mathrm{P}_1)6f$	$^2[3]^0$
79	2.2689594E − 18	18	6	3	1	1/2	4	$2s^2 2p^2(^3\mathrm{P}_1)6f$	$^2[4]^0$
80	2.2689951E − 18	10	6	3	1	1/2	2	$2s^2 2p^2(^3\mathrm{P}_1)6f$	$^2[2]^0$
81	2.2690781E − 18	14	6	2	1	1/2	3	$2s^2 2p^2(^3\mathrm{P})6d$	^{2}F
82	2.2699818E − 18	20	6	2	1	3/2	2	$2s^2 2p^2(^3\mathrm{P})6d$	^{4}D
83	2.2702472E − 18	10	6	2	1	1/2	2	$2s^2 2p^2(^3\mathrm{P})6d$	^{2}D
84	2.2704316E − 18	6	6	3	1	1/2	1	$2s^2 2p^2(^3\mathrm{P}_2)6f$	$^2[1]^0$
85	2.2705093E − 18	22	6	3	1	1/2	5	$2s^2 2p^2(^3\mathrm{P}_2)6f$	$^2[5]^0$
86	2.2705473E − 18	10	6	3	1	1/2	2	$2s^2 2p^2(^3\mathrm{P}_2)6f$	$^2[2]^0$
87	2.2706401E − 18	14	6	3	1	1/2	3	$2s^2 2p^2(^3\mathrm{P}_2)6f$	$^2[3]^0$
88	2.2706620E − 18	18	6	3	1	1/2	4	$2s^2 2p^2(^3\mathrm{P}_2)6f$	$^2[4]^0$
89	2.2753854E − 18	8	7	1	1	3/2	2	$2s^2 2p^2(^3\mathrm{P})7p$	^{4}D°
90	2.2838695E − 18	12	8	0	1	3/2	1	$2s^2 2p^2(^3\mathrm{P})8s$	^{4}P
91	2.2843827E − 18	6	7	2	1	1/2	1	$2s^2 2p^2(^3\mathrm{P})7d$	^{2}P
92	2.2846102E − 18	6	8	0	1	1/2	1	$2s^2 2p^2(^3\mathrm{P})8s$	^{2}P
93	2.2846711E − 18	28	7	2	1	3/2	3	$2s^2 2p^2(^3\mathrm{P})7d$	^{4}F
94	2.2846925E − 18	10	7	2	1	3/2	1	$2s^2 2p^2(^3\mathrm{P})7d$	^{4}P
95	2.2854244E − 18	14	7	2	1	1/2	3	$2s^2 2p^2(^3\mathrm{P})7d$	^{2}F
96	2.2862873E − 18	20	7	2	1	3/2	2	$2s^2 2p^2(^3\mathrm{P})7d$	^{2}D
97	2.2864728E − 18	10	7	2	1	1/2	2	$2s^2 2p^2(^3\mathrm{P})7d$	^{2}D
98	2.2939594E − 18	6	9	0	1	1/2	1	$2s^2 2p^2(^3\mathrm{P})9s$	^{2}P
99	2.2949085E − 18	12	9	0	1	3/2	1	$2s^2 2p^2(^3\mathrm{P})9s$	^{4}P
100	2.2950121E − 18	6	8	2	1	1/2	1	$2s^2 2p^2(^3\mathrm{P})8d$	^{2}P
101	2.2955104E − 18	24	8	2	1	3/2	3	$2s^2 2p^2(^3\mathrm{P})8d$	^{4}F
102	2.2960411E − 18	14	8	2	1	1/2	3	$2s^2 2p^2(^3\mathrm{P})8d$	^{2}F
103	2.2966880E − 18	12	8	2	1	3/2	1	$2s^2 2p^2(^3\mathrm{P})8d$	^{4}P
104	2.2967069E − 18	10	8	2	1	1/2	2	$2s^2 2p^2(^3\mathrm{P})8d$	^{2}D
105	2.2968674E − 18	20	8	2	1	3/2	2	$2s^2 2p^2(^3\mathrm{P})8d$	^{4}D
106	2.3011420E − 18	6	10	0	1	1/2	1	$2s^2 2p^2(^3\mathrm{P})10s$	^{2}P
107	2.3020713E − 18	6	9	2	1	1/2	1	$2s^2 2p^2(^3\mathrm{P})9d$	^{2}P
108	2.3020392E − 18	20	9	2	1	3/2	2	$2s^2 2p^2(^3\mathrm{P})9d$	^{4}D
109	2.3023276E − 18	14	9	2	1	1/2	3	$2s^2 2p^2(^3\mathrm{P})9d$	^{2}F
110	2.3024486E − 18	12	10	0	1	3/2	1	$2s^2 2p^2(^3\mathrm{P})10s$	^{4}P
111	2.3039586E − 18	10	9	2	1	1/2	2	$2s^2 2p^2(^3\mathrm{P})9d$	^{2}D

(continued)

Table A2 Listing of electronic energy level information of atomic nitrogen (Continued)

Level j	$\varepsilon_{\mathrm{el},j}$, J	g_j	n_j	l_j	x_j	S_j	L_j	Configuration	Term
112	2.3040740E − 18	12	9	2	1	3/2	1	$2s^2 2p^2(^3\mathrm{P})9d$	^{4}P
113	2.3063971E − 18	6	11	0	1	1/2	1	$2s^2 2p^2(^3\mathrm{P})11s$	^{2}P
114	2.3067336E − 18	12	11	0	1	3/2	1	$2s^2 2p^2(^3\mathrm{P})11s$	^{4}P
115	2.3073584E − 18	6	10	2	1	1/2	1	$2s^2 2p^2(^3\mathrm{P})10d$	^{2}P
116	2.3074386E − 18	14	10	2	1	1/2	3	$2s^2 2p^2(^3\mathrm{P})10d$	^{2}F
117	2.3075347E − 18	20	10	2	1	3/2	2	$2s^2 2p^2(^3\mathrm{P})10d$	^{4}D
118	2.3090407E − 18	10	10	2	1	1/2	2	$2s^2 2p^2(^3\mathrm{P})10d$	^{2}D
119	2.3094253E − 18	12	10	2	1	3/2	1	$2s^2 2p^2(^3\mathrm{P})10d$	^{4}P
120	2.3098102E − 18	2	3	0	1	1/2	0	$2s^2 2p^2(^1\mathrm{S})3s$	^{2}S
121	2.3103385E − 18	6	12	0	1	1/2	1	$2s^2 2p^2(^3\mathrm{P})12s$	^{2}P
122	2.3104667E − 18	12	12	0	1	3/2	1	$2s^2 2p^2(^3\mathrm{P})12s$	^{4}P
123	2.3112517E − 18	6	11	2	1	1/2	1	$2s^2 2p^2(^3\mathrm{P})11d$	^{2}P
124	2.3114120E − 18	14	11	2	1	1/2	3	$2s^2 2p^2(^3\mathrm{P})11d$	^{2}F
125	2.3115722E − 18	20	11	2	1	3/2	2	$2s^2 2p^2(^3\mathrm{P})11d$	^{4}D
126	2.3129340E − 18	10	11	2	1	1/2	2	$2s^2 2p^2(^3\mathrm{P})11d$	^{2}D
127	2.3130302E − 18	12	11	2	1	3/2	1	$2s^2 2p^2(^3\mathrm{P})11d$	^{4}P
128	2.3135589E − 18	6	13	0	1	1/2	1	$2s^2 2p^2(^3\mathrm{P})13s$	^{2}P
129	2.3142478E − 18	6	12	2	1	1/2	1	$2s^2 2p^2(^3\mathrm{P})12d$	^{2}P
130	2.3158179E − 18	12	12	2	1	3/2	1	$2s^2 2p^2(^3\mathrm{P})12d$	^{4}P
131	2.3166991E − 18	10	12	2	1	1/2	2	$2s^2 2p^2(^3\mathrm{P})12d$	^{2}D

References

[1] Carlson, A. B., and Hassan, H. A., "Radiation Modeling with Direct Simulation Monte–Carlo," *Journal of Thermophysics and Heat Transfer*, Vol. 6, No. 4, 1992, pp. 631–636. doi:10.2514/3.11544

[2] Berghausen, A. K., Taylor, J. C., and Hassan, H. A., "Direct Simulation of Shock Front Radiation in Air," *Journal of Thermophysics and Heat Transfer*, Vol. 10, No. 3, 1996, p. 6. doi:10.2514/3.805

[3] Kossi, K. K., and Boyd, I. D., "Detailed computation of Ultraviolet Spectra in Rarefied Hypersonic Flow," *Journal of Spacecraft and Rockets*, Vol. 35, No. 5, 1998, pp. 653–659. doi:10.2514/2.3381

[4] Park, C., *Nonequilibrium Hypersonic Aerothermodynamics*, Wiley, New York, 1990.

[5] Bird, G. A., "A Comparison of Collision Energy-based and Temperature-Based Procedures in DSMC," *Rarefied Gas Dynamics, 26th Symposium*, Vol. 1084, American Inst. of Physics, Kyoto, Japan, 2009, pp. 245–250.

[6] Gallis, M. A., Bond, R. B., and Torczynski, J. R., "A Kinetic-Theory Approach for Computing Chemical-Reaction Rates in Upper-Atmosphere Hypersonic Flows," *The Journal of Chemical Physics*, Vol. 131, No. 12, 2009, p. 124311. doi:10.1063/1.3241133

[7] Borgnakke, C., and Larsen, P. S., "Statistical Collision Model for Monte Carlo Simulation of Polyatomic Gas Mixtures," *Journal of Computational Physics*, Vol. 18, 1975, pp. 405–420. doi:10.1016/0021-9991(75)90094-7

[8] Bergemann, F., and Boyd, I. D., "New Discrete Vibrational Energy Model for Direct Simulation Monte Carlo Method," *Progress in Astronautics and Aeronautics*, Vol. 160, 1994, pp. 174–183.

[9] Boyd, I. D., "Relaxation of Discrete Rotational Energy Distributions Using a Monte Carlo Method," *Physics of Fluids A*, Vol. 5, No. 9, 1993, pp. 2278–2286. doi:10.1063/1.858531

[10] Bird, G. A., "Monte Carlo Simulation in an Engineering Context," *Progress in Astronautics and Aeronautics*, Vol. 74, No. 1, 1981, pp. 239–255.

[11] Koura, K., and Matsumoto, H., "Variable Soft Sphere Molecular Model for Inverse-Power-Law or Lennard–Jones Potential," *Physics of Fluids A: Fluid Dynamics*, Vol. 3, No. 10, 1991, pp. 2459–2465. doi:10.1063/1.858184

[12] Chernyi, G. G., and Losev, S. A., "Development of Thermal Protection Systems for Interplanetary Flight," Research Institute of Mechanics Rept. No. ISTC 036-96, Moscow, 1999.

[13] Frost, R. M., Awakowicz, P., Summers, H. P., and Badnell, N. R., "Calculated Cross Sections and Measured Rate Coefficients for Electron-Impact Excitation of Neutral and Singly Ionized Nitrogen," *Journal of Applied Physics*, Vol. 84, No. 6, 1998, pp. 2989–3003. doi:10.1063/1.368452

[14] Losev, S. A., Makarov, V. N., Pogosbekyan, M. J., Shatalov, O. P., and Nikol'sky, V. S., "Thermochemical Nonequilibrium Kinetic Models in Strong Shock Waves on Air," AIAA Paper 1994-1990, 1994.

[15] Ozawa, T., Zhong, J., and Levin, D. A., "Development of Kinetic-Based Energy Exchange Models for Noncontinuum, Ionized Hypersonic Flows," *Physics of Fluids*, Vol. 20, 2008. doi:10.1063/1.2907198

[16] Bird, G. A., "Nonequilibrium Radiation During Re-Entry at 10 km/s," AIAA Paper 1987-1543, 1987.

[17] Hash, D., Olejniczak, J., Wright, M., Prabhu, D., Pulsonetti, M., Hollis, B., Gnoffo, P., Barnhardt, M., Nompelis, I., and Candler, G., "FIRE II Calculations for Hypersonic Nonequilibrium Aerothermodynamics Code Verification: DPLR, LAURA and US3D," AIAA Paper 2007-605, 2007.

[18] Boyd, I. D., "Modeling of Plasma Formation in Rarefied Hypersonic Entry Flows," AIAA Paper 2007-206, 2007.

[19] Gupta, R. N., "Navier–Stokes and Viscous Shock-Layer Solutions for Radiating Hypersonic Flows," AIAA Paper 1987-1576, 1987.

[20] Park, C., "Rate Parameters for Electronic Excitation of Diatomic Molecules II. Heavy Particle-Impact Processes," AIAA Paper 2008-1446, 2008.

[21] Guerra, V., and Loureiro, J., "Electron and Heavy Particle Kinetics in a Low-Pressure Nitrogen Glow Discharge," *Plasma Sources Science and Technology* , Vol. 6, No. 3, 1997, pp. 361–372. doi:10.1088/0963-0252/6/3/013

[22] Levin, D. A., "Modeling of VUV Radiation at High Altitudes," AIAA Paper 1996-1899, 1996.

A. Ketsdever
Associate Editor